

# Production of Eco-Friendly Blended Calcium Sulfoaluminate Cements by Using Biomass-Fly Ashes

Milena Marroccoli<sup>a,\*</sup>, Francesco Laguardia<sup>a</sup>, Marco De Biasi<sup>a</sup>, Antonio Telesca<sup>a</sup>

<sup>a</sup>Scuola di Ingegneria, Università degli Studi della Basilicata, Viale dell'Ateneo Lucano 10, Potenza 85100, Italia

\*[milena.marroccoli@unibas.it](mailto:milena.marroccoli@unibas.it)

The manufacture of Ordinary Portland cement (OPC) generates about 8% of all anthropogenic CO<sub>2</sub> emissions; therefore, carbon dioxide footprint reduction represents the main challenge for the cement industry. The development of environmentally friendly binders, as alternative to OPC, absolutely represents an efficient way to cut carbon emissions. In this regard, during the last twenty years particular attention has been paid to calcium sulfoaluminate (CSA) cements thanks to their valuable technical properties as well as the environmentally friendly features mainly related to their manufacturing process. In addition, a further reduction in carbon dioxide emissions can be achieved diluting CSA cements with supplementary cementitious materials (SCMs) such as industrial wastes. In this title, biomass fly ashes (BFAs) were used as SCMs in CSA-blended cements; BFAs were preliminarily washed (W\_BFAs) in order to lower their content in alkali. The influence of the ashes on both hydration properties and technical behaviour of two CSA blended cements, respectively containing 10% and 20% by mass of W\_BFAs, was investigated by means of mechanical compressive strength and dimensional stability measurements associated with X-ray diffraction, differential thermal-thermogravimetric and mercury intrusion porosimetric analyses.

## 1. Introduction

In 2019 global cement production was about 4.1 billion tonnes; in the same year the total carbon dioxide generated by cement plants reached almost 3.0 billion tonnes, accounting for nearly 8% of all anthropogenic CO<sub>2</sub> emissions (IEA, 2020, Tregambi et al. 2018). Therefore, the main challenge for the cement industry is to curb its carbon footprint; to this end, both cement producers and scientific community have suggested several solutions, such as: a) a larger utilization of alternative fuels; b) the application of carbon capture and storage technologies to cement plants and c) the development of alternative eco-friendly binders (EFBs) (Telesca et al., 2016); EFBs can be produced following three different approaches, namely I) the use of a non-carbonated CaO source instead of limestone as a constituent of the raw mixture for the generation of the burnt product (cement clinker); II) the increased production of blended cements, obtained by adding significant amounts of supplementary cementitious materials (SCMs) (Telesca et al., 2017) to traditional ordinary Portland cements (OPCs); III) a greater utilization of special binders (e.g. Mg-based cements, alkali-activated, calcium sulfoaluminate (CSA) and belite-CSA (BCSA) binders) (Luukkonen et al., 2018; Telesca et al., 2020; Walling and Provis, 2016).

CSA cements have attracted the interest of the international cement community thanks to their valuable technical properties as well as the eco-friendly features of their manufacturing process (Gartner et al., 2015; Marroccoli et al., 2009; Marroccoli et al., 2010a; Marroccoli et al., 2010b; Telesca et al., 2016; Telesca et al., 2019a; Telesca et al., 2019b). 3CaO·3Al<sub>2</sub>O<sub>3</sub>·CaSO<sub>4</sub> is the main mineralogical component of CSA cements; furthermore, they can also contain calcium sulfates, 2CaO·SiO<sub>2</sub>, 4CaO·Al<sub>2</sub>O<sub>3</sub>·Fe<sub>2</sub>O<sub>3</sub>, 4CaO·2SiO<sub>2</sub>·CaSO<sub>4</sub> and various calcium aluminates, depending on the synthesis temperature as well as type and proportioning of raw materials. The CSA technical properties (e.g. rapid setting, high early strength, shrinkage compensation/self-stressing behaviour, good dimensional stability, elevated impermeability,) mainly depend on the formation of ettringite (3CaO·Al<sub>2</sub>O<sub>3</sub>·3CaSO<sub>4</sub>·32H<sub>2</sub>O) which forms through the hydration of CaSO<sub>4</sub> (belonging and/or added

to CSA clinker) with  $3\text{CaO}\cdot 3\text{Al}_2\text{O}_3\cdot \text{CaSO}_4$  (Chen et al., 2012; Glasser and Zhang, 2001; Winnefeld and Lothenbach, 2010; Marroccoli et al., 2007). In addition, compared to OPC, the manufacturing process of CSA cements occurs at lower synthesis temperatures ( $<1350^\circ\text{C}$ ) and requires a reduced limestone amount ( $<40\%$ ); consequently, fewer fossil fuels are consumed and  $\text{CO}_2$  emissions are reduced. In order to further lower the carbon footprint and cut the high costs of production (largely depending on the use of bauxite in the generating raw meal), CSA cements can be mixed with proper SCMs (Garcia-Mate et al., 2013; Lukas et al., 2017; Martin et al., 2015; Pelletier-Chaignat et al., 2012). The addition of biomass fly ashes (BFAs) to OPC has been documented in several scientific articles (Berra et al., 2015; Rajamma R.J.B. R. 2009; Rajamma et al., 2015; Siddique, R., 2012; Tosti et al., 2018). BFAs usually come out from the combustion process of wood, agriculture wastes and herbaceous biomass in thermal power plants. The chemical and mineralogical composition of BFAs depend on the biomass characteristics as well as the combustion technology; they are generally landfilled (van Eijk et al., 2012) or used in forest agricultural fields (Kwapinski et al., 2010) owing to their high alkali content. This paper aimed to investigate the use of BFAs, formerly submitted to an alkali reduction treatment by means of a water-washing process (WWP), as SCMs in CSA blended-cements; these binders were submitted to physical-mechanical and hydration tests for aging periods comprised in the range 4 hours - 56 days. X-ray diffraction (XRD) and differential-thermal thermogravimetric (DT-TG) analyses coupled with mercury intrusion porosimetry (MIP) were employed as main characterization techniques.

## 2. Experimental program

A commercial CSA cement, supplied by an Italian cement manufacturer, was used for this study. BFAs samples were collected from the baghouse filter of a thermal power plant burning woodchips located in Basilicata Region (ITALY). Table 1 reports the chemical composition of both materials, evaluated by means of X-ray fluorescence analysis (BRUKER Explorer S4 apparatus); a BRUKER D2 PHASER diffractometer ( $\text{CuK}\alpha$  radiation and  $0.02^\circ 2\theta \text{ s}^{-1}$  scanning rate) was utilized for the identification of the main mineralogical phases of BFAs and CSA cement. The Rietveld refinement (carried out through the TOPAS software, Table 1) was employed only for the quantitative mineralogical determination of CSA cement. Due to the high alkali content, ( $\text{Na}_2\text{O}$  and  $\text{K}_2\text{O}$ ), BFAs underwent a WWP using a distilled water/BFAs equal to 10. The washing process was carried out by means of a magnetic stirrer at 1500 rpm for 2 hours at room temperature. The chemical composition of “washed BFAs (W\_BFAs)” is shown in Table 1 which also reports the specific gravity values (estimated with a pycnometer) and the specific surface (measured according to EN 196-6) of the investigated materials.

*Table 1: Chemical, mineralogical composition and physical properties of the binder components*

	Chemical composition (wt%)			Mineralogical phase composition (wt%)		
	CSA cement	BFAs	W_BFAs	CSA cement	ICDD reference number	
CaO	44.58	40.09	42.20	Ye'elimite	30-0256	43.0
SiO <sub>2</sub>	8.95	26.30	27.68	$\beta$ -belite	33-0302	21.7
Al <sub>2</sub> O <sub>3</sub>	22.42	6.82	7.18	Celite	38-1429	3.8
Fe <sub>2</sub> O <sub>3</sub>	1.86	3.04	3.20	Anhydrite	37-1496	19.1
TiO <sub>2</sub>	1.10	0.34	0.36	Calcite	05-0586	1.1
K <sub>2</sub> O	0.30	7.38	3.62	Brownmillerite	30-0256	4.5
MnO	0.08	0.19	0.19	Gehlenite	73-2041	1.6
Na <sub>2</sub> O	0.08	2.08	1.25	Others		5.2
MgO	0.94	3.09	4.20			
Cl <sup>-</sup>	0.07	1.02	0.23			
SO <sub>3</sub>	16.85	2.07	2.18			
P <sub>2</sub> O <sub>5</sub>	0.05	3.38	3.40			
I.o.i.*	2.16	4.09	4.30			
Total	99.44	99.89	99.99	Total		100.0
Specific gravity (g/cm <sup>3</sup> )	3.11	2.57	2.51			
Specific surface (cm <sup>2</sup> /g)	4500±50		4800±50			

\*I.o.i.=loss on ignition measured at  $950^\circ\pm 10^\circ\text{C}$

W\_BFAs were also submitted to XRD analysis; the EVA software was employed for the evaluation of both patterns and amorphous content of BFAs and W\_BFAs. Two CSA blended cements (CSA\_10 and CSA\_20), respectively containing 10% and 20% by mass of W\_BFAs, were investigated; a plain CSA cement (CSA\_R) was used as a reference term. For each system, twenty-one mortar prisms were prepared according to the European Standard EN 196-1. After demolding, with the exception of the samples cured for 4 and 24 hours, mortar prisms were placed under water at  $20^\circ\pm 1^\circ\text{C}$  until compressive mechanical strength test was carried out

(at 4 and 24 hours and 2, 7, 28 and 56 days). A 0.50 water/solid mass ratio was employed for the preparation of CSA-based cement pastes; they were cast into small plastic vessels and positioned in a thermostatic bath at room temperature for aging periods from 4 hours up to 56 days. At the end of each aging period, every specimen was broken in half: one part was submitted to MIP analysis, the other was finely pulverized (grain size  $<63\mu\text{m}$ ) for XRD and DT–TG measurements. Both the hardened fragments and powders were primary treated with acetone (to stop hydration) and diethyl ether (to remove water) and then stored in a desiccator containing silica gel and soda lime (to ensure protection against  $\text{H}_2\text{O}$  and  $\text{CO}_2$ , respectively). Six prisms paste samples (15X15X78 mm) were submitted to dimensional stability test; the prisms were cured in air at room temperature for 4 hours and then demolded. Three samples were aged at  $20^\circ\text{C}$  under tap water, the others were stored in a chamber at 50% R.H. and  $20^\circ\text{C}$ . Length changes were determined as average values of three measurements taken with a length comparator apparatus.

### 3. Results and discussion

Ye'elimite was the main phase of CSA cement (43.0 wt%); belite and calcium sulfate, mainly deriving from the addition of natural anhydrite, were present as secondary components. BFAs were “high-calcium biomass fly-ashes” owing to their high content in CaO (40.09 wt%) with regard to  $\text{SiO}_2$  amount (26.30 wt%); the ashes were also rich in  $\text{K}_2\text{O}$  (7.38 wt%) and low in (I)  $\text{Na}_2\text{O}$  (2.08 wt%), (II)  $\text{SO}_3$  (2.07 wt%) and (III) Cl (1.02 wt%). After the WWP, W\_BFAs were much lower in alkalis ( $\text{Na}_2\text{O}_{\text{eq}}=3.64$  wt%). XRD analysis revealed that quartz, mullite, hematite and  $\text{CaO}_f$  (free CaO) were the main crystalline phases for both BFAs and W\_BFAs; additionally, their amorphous content was equal to 45 wt% and 48 wt%, respectively. The time development of mechanical compressive strength of the three systems is reported in Figure 1.

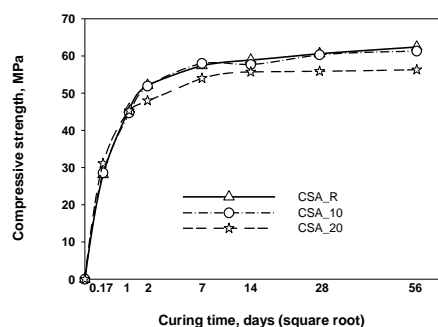


Figure 1: Compressive strength values for CSA\_R, CSA\_10 and CSA\_20 cured at various periods.

For all the investigated curing periods, it was found that: a) the compressive strength for CSA\_R and CSA\_10 based-mortars were almost similar to each other; b) CSA\_20 based-mortar, compared with the afore mentioned systems, exhibited compressive strength values higher after 4 hours of hydration, almost equal after 1 day and about 8% lower at curing periods longer than 14 days.

Figure 2 shows the length change vs. curing time for the three systems; they differed very little from each other, both when submerged under water and cured in air.

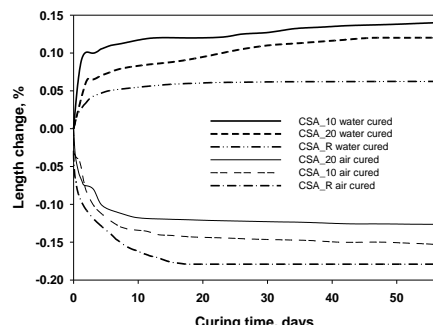


Figure 2: Dimensional stability curves for CSA-based cements (air and water cured).

The maximum expansion values, comprised in the narrow range 0.06-0.19%, were reached after about 14 days of curing for the samples cured under water; on the contrary, the pastes cured in air exhibited a continuous shrinkage until 14 days when a minimum length change was reached (-0.17%, -0.15% and -0.13% for CSA\_R, CSA\_10 and CSA\_20, respectively). Figure 3 displays the DT results for CSA\_R, CSA\_10 and CSA\_20

hydrated for different curing times (4 and 24 hours, 7, 28 and 56 days). With DT–TG temperature increase, three different endothermic effects were identified (at  $109^{\circ}\pm 4^{\circ}\text{C}$ ,  $166^{\circ}\pm 4^{\circ}\text{C}$  and  $285^{\circ}\pm 2^{\circ}\text{C}$ ) and attributed, in the order, to the following hydration products (Taylor,1997):  $\text{CaO}\cdot\text{SiO}_2\cdot\text{H}_2\text{O}$ ,  $3\text{CaO}\cdot\text{Al}_2\text{O}_3\cdot 3\text{CaSO}_4\cdot 32\text{H}_2\text{O}$  and  $\text{Al}_2\text{O}_3\cdot 3\text{H}_2\text{O}$ ; furthermore, except for the peak related to  $\text{CaCO}_3$  present in  $\text{W\_BFAs}$ , no significant effects were found above  $500^{\circ}\text{C}$ .

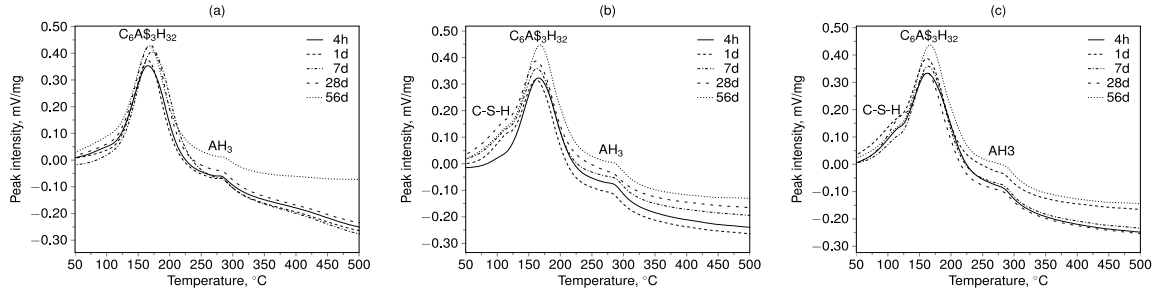


Figure 3: DT results for CSA\_R (a), CSA\_10 (b) and CSA\_20 (c) hydrated for 4 hours, 1, 7, 28 and 56 days. Legend:  $\text{CaO}\cdot\text{SiO}_2\cdot\text{H}_2\text{O}=\text{C-S-H}$ ;  $3\text{CaO}\cdot\text{Al}_2\text{O}_3\cdot 3\text{CaSO}_4\cdot 32\text{H}_2\text{O}=\text{C}_6\text{A}_3\text{H}_{32}$ ;  $\text{AH}_3=\text{Al}_2\text{O}_3\cdot 3\text{H}_2\text{O}$ .

On the whole, the DT results revealed the presence of  $3\text{CaO}\cdot\text{Al}_2\text{O}_3\cdot 3\text{CaSO}_4\cdot 32\text{H}_2\text{O}$  and  $\text{Al}_2\text{O}_3\cdot 3\text{H}_2\text{O}$  for all the curing periods while  $\text{CaO}\cdot\text{SiO}_2\cdot\text{H}_2\text{O}$  was detected only in the systems containing  $\text{W\_BFAs}$  thanks to the hydration of their reactive  $\text{CaO}$  and  $\text{SiO}_2$ ; furthermore, both  $3\text{CaO}\cdot\text{Al}_2\text{O}_3\cdot 3\text{CaSO}_4\cdot 32\text{H}_2\text{O}$  and  $\text{Al}_2\text{O}_3\cdot 3\text{H}_2\text{O}$  concentrations increased with aging time. In general, these outcomes suggested that: I) the hydration behavior of  $\text{CSA\_R}$  are chiefly regulated by the reaction of ye’elite with calcium sulfate; II) the hydraulic performances of both  $\text{CSA\_10}$  and  $\text{CSA\_20}$  also depend on the self-cementing properties of  $\text{W\_BFA}$  reactive components. The hydration evolution for the three systems was also evaluated in terms of chemically bound water (Figure 4) calculated on the basis of the mass loss values (up to  $500^{\circ}\text{C}$ ) from TG analyses.

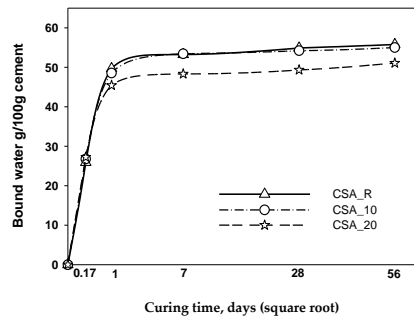


Figure 4. Bound water as determined up to 56 days of hydration (normalized to 100g of anhydrous cement) for  $\text{CSA\_R}$ ,  $\text{CSA\_10}$  and  $\text{CSA\_20}$  plotted against curing time.

Figure 4 indicates that the three systems followed a similar trend in terms of hydration process evolution; additionally, except for  $\text{CSA\_20}$ , the other binders reached comparable bound water values at 56 days of curing. XRD outcomes confirmed the indications given by DT-TG analyses. From these results it can be ascertained that the hydraulic activity of  $\text{W\_BFAs}$  does not influence the mechanical properties of  $\text{CSA\_10}$ , while only a low decrease of the compressive strength is shown when 20% of biomass ash was added to  $\text{CSA}$  cement; these findings are confirmed by MIP investigations.

Figure 5 displays the porosimetric curves for hydrated cement pastes of the investigated systems; the top and the bottom part of the Figure respectively reports the cumulative and derivative plots for intruded  $\text{Hg}$  volume of  $\text{CSA}$ -based cements vs. pore radius at various curing times (from 4 hours to 56 days). A unimodal pore size distribution, centred on the lowest width of pore necks connecting a continuous system, is observed for  $\text{CSA\_R}$  (Figure 5 (a)) at all the curing periods [6]; in particular, with the increase of curing time, both cumulative pore volume and threshold pore width respectively decrease from 225 to 120  $\text{mm}^3/\text{g}$  and from about 210 to 20 nm. In comparison to  $\text{CSA\_R}$ , the other two systems show a different behaviour: a multimodal pore size distribution, already present after 4 hours of hydration, is found at all the investigated curing times; moreover, for  $\text{CSA\_10}$ , due to high reaction rate, the cumulative pore volume reduces of about 37% (from 258 to 162  $\text{mm}^3/\text{g}$ ) from 4 hours to 2 days; on the contrary, at longer curing times, this value is almost constant ( $\sim 108 \text{ mm}^3/\text{g}$ ). At the earliest and longest curing times, the first and the last thresholds pore widths respectively shift from 400 to 118 nm and from 5 to less than 3.6 nm. Similar porosimetric features are also observed for  $\text{CSA\_20}$  system.

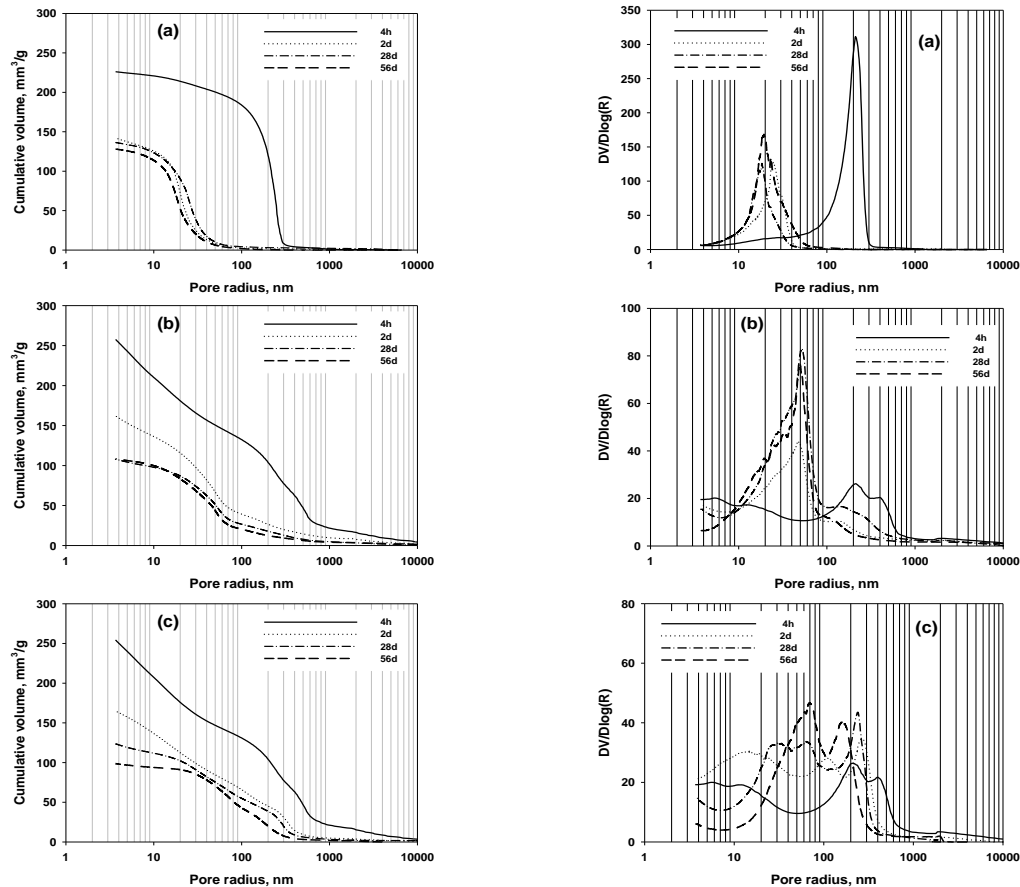


Figure 5: Cumulative (left) and derivative (right) Hg volume vs. pore radius for CSA\_R (a), CSA\_10 (b) and CSA\_20 (c) pastes cured from 4 hours to 56 days.

#### 4. Conclusions

In this paper the possibility of using biomass fly ashes (BFAs), as alternative supplementary cementitious materials (SCMs) in calcium sulfoaluminate (CSA)-blended cements, was evaluated. BFAs were first submitted to a water washing process (W\_BFAs) with the aim of reducing the high alkali content. W\_BFAs are very interesting since their utilization as SCMs, in addition to the saving of raw materials and waste landfilling, allows the CSA cement dilution which implies both a decreased emission of CO<sub>2</sub> and a noticeable energy saving per unit mass of manufactured cement. W\_BFAs were mainly composed by reactive calcium-, silicon- and aluminum-oxides which react with water to give calcium silicate hydrate responsible for its binder properties. On the whole, the experimental results demonstrated that the use of W\_BFAs (up to 20% by mass) in CSA-blended cements did not appreciably influence mortars compressive mechanical strength, pastes dimensional stability and hydration behaviour.

#### References

- IEA, 2020. <https://www.iea.org/reports/global-energy-review-2020/global-energy-and-co2-emissions-in-2020>. Last accessed: December 2020.
- Berra M., Mangialardi T., Paolini A.E., 2015, Reuse of Woody Biomass Fly Ash in Cement-Based Materials, *Construction and Building Material*, 76, 286–296. DOI: 10.1016/j.conbuildmat.2014.11.052
- Chen I.A., Hargis C.W., Juenger M.C.G., 2012, Understanding Expansion in Calcium Sulfoaluminate-Belite Cements, *Cement and Concrete Research*, 42(1), 51–60. DOI:10.1016/j.cemconres.2011.07.010
- Garcia-Mate M., De la Torre A.G., Leon-Reina L., Aranda M.A.G., Santacruz I., 2013, Hydration Studies of Calcium Sulfoaluminate Cements Blended with Fly Ash, *Cement and Concrete Research*, 54, 12–20. DOI:10.1016/j.cemconres.2013.07.010
- Gartner E., Hirao H., 2015, A Review of Alternative Approaches to the Reduction of CO<sub>2</sub> Emissions Associated with the Manufacture of the Binder Phase in Concrete, *Cement and Concrete Research*, 78, 126–142. DOI:10.1016/j.cemconres.2015.04.012

- Glasser F.P., Zhang L., 2001, High-Performance Cement Matrices Based on Calcium Sulphoaluminate-Belite Compositions, *Cement and Concrete Research*, 31(12), 1881–1886. DOI: 10.1016/S0008-8846(01)00649-4
- Kwapinski W., Byrne C.M.P., Kryachko E., Wolfram P., Adley C., Leahy J.J., Novotny E.H., Hayes M.H.B., 2010, Biochar from Biomass and Waste, *Waste Biomass Valorization*, 77–89. DOI:10.1007/s12649-010-9024-8
- Lukas H.J., Winnefeld F., Tschopp E., Müller C.J., Lothenbach B., 2017, Influence of Fly Ash on the Hydration of Calcium Sulfoaluminate Cement, *Cement and Concrete Research*, 95, 152-163. DOI:10.1016/j.cemconres.2017.02.030
- Luukkonen T., Abdollahnejad Z., Yliniemi J., Kinnunen P., Illikainen M., 2018, One-Part Alkali-Activated Materials: A Review, *Cement and Concrete Research*, 103, 21–34. DOI:10.1016/j.cemconres.2017.10.001
- Marroccoli M., Nobili M., Telesca A., Valenti G.L., 2007, Early Hydration of Calcium Sulfoaluminate-Based Cements for Structural Applications, *Int. Conf. Sust. Constr. Mat. Tech.*, Coventry, United Kingdom, 389-395.
- Marroccoli M., Montagnaro F., Pace M.L., Valenti G.L., 2009, Use of Fluidized Bed Combustion Ash and Other Industrial Wastes as Raw Materials for the Manufacture of Calcium Sulphoaluminate Cements, 20<sup>th</sup> Int. Conf Fluid. Bed Comb., Xian, China, 389–395.
- Marroccoli M., Pace M.L., Telesca A., Valenti G.L., 2010a, Synthesis of Calcium Sulfoaluminate Cements from Al<sub>2</sub>O<sub>3</sub>-Rich Byproducts from Aluminium Manufacture, 2<sup>nd</sup> Int. Conf. Sust. Constr. Mat. Tech., Ancona, Italy, 615-623.
- Marroccoli M., Montagnaro F., Telesca A., Valenti G.L., 2010b, Environmental Implications of the Manufacture of Calcium Sulfoaluminate-Based Cements, 2<sup>nd</sup> Int. Conf. Sust. Constr. Mat. Tech., Ancona, Italy, 625-635.
- Martin L.H.J., Winnefeld F., Müller C.J., Lothenbach B., 2015, Contribution of Limestone to the Hydration of Calcium Sulfoaluminate Cement, *Cement and Concrete Composite*, 62, 204–211.
- Pelletier-Chaignat L., Winnefeld F., Lothenbach B., Müller C.J., 2012, Beneficial Use of Limestone Filler with Calcium Sulfoaluminate Cement, *Construction and Building Materials*, 26, 619-627. DOI:10.1016/j.conbuildmat.2011.06.065
- Rajamma R., Senff L., Ribeiro M.J., Labrincha J.A., Ball R.J., Allen G.C., Ferreira V.M., 2015. Biomass Fly Ash Effect on Fresh and Hardened State Properties of Cement-Based Materials. *Composites Part B: Engineering*, 77, 1–9. DOI:10.1016/j.compositesb.2015.03.019
- Rajamma R.J.B.R., 2009. Characterisation and Use of Biomass Fly Ash in Cement-Based Materials, *Journal of Hazardous Materials*, 172, 1049–1060. DOI:10.1016/j.jhazmat.2009.07.109
- Siddique R., 2012, Utilization of Wood Ash in Concrete Manufacturing, *Research, Construction and Recycling*, 67, 27–33. DOI:10.1016/j.resconrec.2012.07.004
- Taylor H.F.W., 1997. *Cement Chemistry*, Academic Press Publisher, London, UK, 436.
- Telesca A., Marroccoli M., Tomasulo M., Valenti G.L., Dieter H., Montagnaro F., 2016, Low-CO<sub>2</sub> Cements from Fluidized Bed Process Wastes and Other Industrial Byproducts, *Combustion Science and Technology*, 188, 492–503. DOI:10.1080/00102202.2016.1138736.
- Telesca A., Marroccoli M., Ibris N., Lupiáñez C., Díez L.I., Romeo L.M., Montagnaro F., 2017, Use of Oxyfuel Combustion Ash for the Production of Blended Cements: A synergetic Solution Toward Reduction of CO<sub>2</sub> Emissions, *Fuel Processing and Technology*, 156, 211–220. DOI:10.1016/j.fuproc.2016.10.026
- Telesca A., Marroccoli M., Winnefeld F., 2019a, Synthesis and Characterization of Calcium Sulfoaluminate Cements Produced by Different Chemical Gypsums, *Advances in Cement Research*, 31(3), 113–123. DOI:10.1680/jadcr.18.00122
- Telesca A., Mobili A., Tittarelli F., Marroccoli M., 2019b, Calcium Sulfoaluminate Cement and Fly Ash-based Geopolymer as Sustainable Binders for Mortars. *Chemical Engineering Transaction*, 74, 1249-1254 DOI:10.3303/CET1974209
- Telesca A., Matschei T., Marroccoli M., 2020, Study of Eco-Friendly Belite-Calcium Sulfoaluminate Cements Obtained from Special Wastes, *Applied Sciences*, 10, 8650. DOI:10.3390/app10238650
- Tosti L., van Zomeren A., Pels J.R., Comans R.N.J., 2018, Technical and Environmental Performance of Lower Carbon Footprint Cement Mortars Containing Biomass Fly Ash as a Secondary Cementitious Material, *Resources, Conservation and Recycling*, 134, 25–33. DOI:10.1016/j.resconrec.2018.03.004
- Tregambi C., Solimene R., Montagnaro F., Salatino P., Marroccoli M., Ibris N., Telesca A., 2018, Solar-Driven Production of Lime for Ordinary Portland Cement Formulation, *Solar Energy*, 173, 759–768. DOI:10.1016/j.solener.2018.08.018
- van Eijk R.J., Obernberger I., Supancic K., 2012, Options for Increased Utilization of Ash from Biomass Combustion and Co-Firing (No. 30102040- PGR/R& E 11-2142)', IEA Bioenergy Task 32.
- Walling S.A., Provis J.L., 2016, Magnesia-Based Cements: A Journey of 150 Years, and Cements for the Future?, *Chemical Reviews*, 116, 4170–4204. DOI:10.1021/acs.chemrev.5b00463
- Winnefeld F., Lothenbach B., 2010, Hydration of Calcium Sulfoaluminate Cements: Experimental Findings and Thermodynamyc Modelling, *Cement and Concrete Research*, 40(8), 1239-1247. DOI:10.1016/j.cemconres.2009.08.014